Ultramicroscopy 52 (1993) 404–414
North-Holland

ultramicroscopy

The defocus contrast of a θ' precipitate in Al–4wt%Cu: Fresnel fringe analysis applied to an atomically abrupt interface

R.E. Dunin-Borkowski and W.M. Stobbs

Department of Materials Science and Metallurgy, University of Cambridge, Pembroke Street, Cambridge CB2 3QZ, UK

Received 5 January 1993

Dedicated to Professor John M. Cowley on the occasion of his seventieth birthday

The through-focal contrast of a θ' precipitate in Al–4wt%Cu is examined. The aim of the work presented here is to establish whether Fresnel contrast analysis can be used to characterise an atomically abrupt interface. Simulations are presented which illustrate the sensitivity of variations in image contrast, at relatively low resolution and as a function of the defocus, to atomically localised changes in compositional spread. The effects of dynamical contributions to the contrast variations are also considered in this context. Preliminary experimental data are analysed and the problems associated with matching experiment and theory are discussed.

1. Introduction

The Fresnel method appears to be a powerful method for determining the compositional profiles of interfaces to the atomic level, by making use of the contrast trends present in relatively low resolution focal series of the edge-on boundaries [1]. Using in general weak diffraction conditions, the technique has been applied, apparently successfully, to problems as diverse as grain boundary segregation in aluminium alloys and the quantification of the surprisingly diffuse interfaces in MBE grown GaAs/AlAs heterostructures [2]. No genuinely atomically discrete interface has yet been analysed, and until this has been done doubts are bound to remain about the interpretation.

Our present investigation has thus had two aims. The first has been to establish whether an atomically abrupt interface, as might be expected to be present at a θ' interface, can be characterised using the Fresnel method as previously applied, or whether the technique needs to be used in new ways for such genuinely discrete boundaries. The second aim has been to gain an understanding of the sensitivity of the approach to changes in composition profile when there are strong dynamical contributions to the contrast. The approach we have taken in both contexts has been to examine the effect of changes in the interface diffuseness on simulations of both diffraction patterns and images as a function of specimen orientation. Such an examination of the reciprocal space information included in an objective aperture of a given size should provide an insight into the reliability of interpretations beyond the resolution limit in a given image. There are potential advantages in using Fresnel fringe analysis at relatively low resolution for determining a compositional profile in that, for example, the effects of the phase changes caused by the objective lens on the relatively coarser detail in a low resolution image are more reliably defined than they are for higher image resolution. However, it remains a central concern that high resolution information about the interface is, in fact, retained within the small objective aperture used. The work described here is thus part of a more broad ranging investigation of this point.

We have chosen to examine edge-on θ' platelets in Al–4wt%Cu specifically because their interfaces are expected to be atomically abrupt.

SSDI 0304-3991(93)E0105-H

Information about the structure will be spread further in reciprocal space for an abrupt than for a diffuse interface, but the effect of this on low resolution Fresnel fringe contrast is not clear. However, it seems reasonable that dynamical scattering back into the small objective aperture used would be a requirement for reliable measurement of interface "shape" at resolutions beyond those of the individual images used. Dynamical effects will be strong at and around the matrix cube normal, given the θ' orientation relation and the large value of $(002)_{\theta'}$ which leads to a large number of reflections at low angles for the edge-on platelets. Given that most of the systems that have been characterised to date using the Fresnel method have been examined under conditions for which diffracted beams have been at relatively high angles, it is a specific interest of the work described here to see whether dynamical contributions between lower angle beams make the profiling easier or more difficult. Some of the problems associated with analysing Fresnel fringes in the presence of strong diffraction contrast have already been demonstrated for Ω precipitates in the Al–Cu–Mg–Ag system [3]. It was found that the contrast was complicated, depending dynamically upon both foil and precipitate thickness, and that the precipitate strain field induced diffraction contrast in the matrix which affected the Fresnel contrast behaviour. Nonetheless, chemical profiling still proved to be possible for this system at a matrix systematic row orientation [4].

For a number of reasons the analysis of a θ' interface profile is a difficult problem, and can be treated as a limiting test case. As well as there being the complications associated with strong dynamical contrast (as noted above), the mean forward scattering potential difference ΔV of 0.51 V is small when compared to that of most of the systems already analysed. The value of ΔV between GaAs and AlAs is, for example, 1.35 V [2]. For larger apertures the contrast may be further complicated by the presence of moiré fringes originating from interference between θ' 004 and aluminium 002 reflections, given the image spreading associated with the large defoci needed.

We will start the description of our results with an examination of the sensitivity of a range of simulations, as a function of the orientation relative to the cube normal, to the compositional diffuseness of the θ' interface. We then proceed to a preliminary investigation of an experimental series of images in order to demonstrate the real difficulties that we are up against.

2. Unit cell and simulation details

θ' has the $CuAl_2$ composition, is tetragonal with $a = 0.405$ nm and $c = 0.58$ nm, and consists of alternate layers of Al and Cu atoms on $(001)_{\theta'}$ planes. The precipitate grows as thin plates on {001} planes in the aluminium-rich matrix, so that (001) matrix and precipitate planes are parallel. The broad faces are completely coherent, while the edges of the plates have a large misfit.

The atomistic multislice simulations used in this paper incorporated Doyle and Turner scattering factors [5] and were carried out at 50 kV and at 200 kV for JEOL 2000FX microscope parameters (see below) and for typical experimental conditions. The supercells used were sampled in real space at 0.012 nm/pixel and had dimensions of 25 nm by 0.405 nm, the long dimension of which was large enough to prevent wraparound of fringes. A sensible form of the compositional spread at matrix/precipitate interfaces proved to be difficult to incorporate, because simply interchanging Cu and Al atoms necessitated also modifying the interlayer spacings. It was decided to model a linearly graded profile for the mean forward scattering potential V_0 by introducing fractional Cu atom vacancies at the edges of the θ' plates. Only a 10% change in Cu occupancy is needed to reduce the θ' forward scattering potential to that for aluminium. The simulations presented here do not include the effects of accommodating the precipitate elastically in the matrix. Experimentally, θ' plates have been observed to exhibit a sequence of misfits as they thicken [6]. Most plates of thickness greater than 3 nm were interstitial, with the elastically accommodated misfit taking a minimum value for matched structural units of the two phases. In the context of this paper the effects of the associated

disregistry of the Al cube planes are unimportant; we are concerned primarily with how the minimal grading indicated above might affect the diffraction behaviour and Fresnel contrast in images obtained using objective apertures which exclude the higher scattering angles at which the primary kinematic changes caused by atomistically localised grading changes will occur.

3. Simulations

Here we compare the diffraction behaviour of a θ' platelet with abrupt interfaces with that for one with both interfaces linearly graded over a single θ' half-unit cell in the manner outlined above. We do not of course suggest that it would be useful to quantify experimental diffraction patterns in this context. Our interest is in whether or not there are changes in the simulated dynamical diffraction patterns due to atomically localised changes in the compositional spread within the low angles that would be accepted when forming a Fresnel series of images. In order to clarify the origins of any such change the simulated diffraction patterns, as well as the image behaviour, are examined as a function of crystal tilt from the matrix cube normal about the platelet $(001)_{\theta'}$ normal. This takes us through a series of differing strongly dynamical contrast conditions towards the more standard Fresnel imaging condition in which only a systematic row of reflections is strongly excited. Fig. 1 allows a comparison of diffraction patterns for the different models, which have been calculated at 200 kV and plotted on a logarithmic scale for three different crystal tilts from [100] about [001]. The θ'/matrix interfaces have been kept vertical throughout. Fig. 2 shows an equivalent set of diffraction patterns, now calculated at 50 kV, so that the reduced radius of the Ewald sphere should alter the relative dynamical effects for the two phases. At 200 kV (fig. 1) it can be seen that the effect of the crystal tilt has been to strengthen the $(000)_{Al}$ reflection, but to weaken the more diffuse central maximum for the θ'. It is also significant that changes are clear in the shoulder of the $(000)_{\theta'}$ reflection, particularly at a tilt of 2.1°. At 50 kV

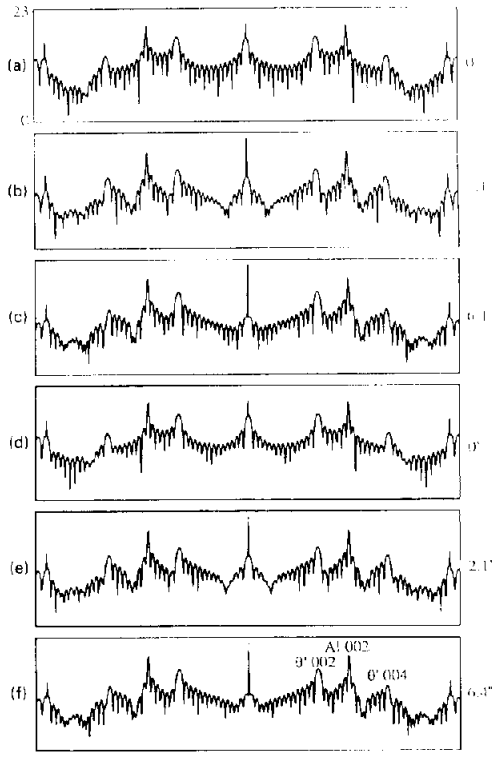

Fig. 1. Traces across systematic row in simulated 200 kV diffraction patterns for 4.4 nm thick (001) θ' precipitate in aluminium. Graphs are plotted on natural log scale, at tilts from [100] indicated. (a), (b) and (c) are for abrupt interface; (d), (e) and (f) are for compositional spread over one θ' half-unit cell.

(fig. 2) changes in the $(000)_{Al}$ beam are less evident though we can again see changes in the shape of the $(000)_{\theta'}$ reflection. The very variable behaviour of the shape of the $(000)_{\theta'}$ beam will have its origin in changes in the dynamical scattering for the θ' reflections. Different subsidiary maxima will intersect the Ewald sphere with differing effects on the shape of the $(000)_{\theta'}$ reflection for small changes in crystal tilt. This is exemplified in fig. 3.

Fig. 4 shows the absolute differences of the diffraction patterns for the discrete and diffuse interface models, again on a logarithmic scale. These are plotted in order to see the effects of compositional spread in the simulated diffraction patterns more clearly. The graphs highlight how

misleading it can be to compare the diffraction patterns themselves on a logarithmic scale, where small differences can be accentuated in regions where the absolute intensities are low. Nonetheless, it is also clear that the changes caused by a change in compositional spread are very small. This is why the Fresnel method has to be used to amplify their effect in a defocus series of images. From fig. 4 it can be seen that there are differences in the $(000)_{\theta'}$ shoulder at all tilts, and that these differences are comparable near to the origin, whatever the tilt, at 50 kV, but decrease with tilt more strongly at 200 kV. This is encouraging in relation to our concern over the degree to which Fresnel data obtained with a small objective aperture can allow us to infer information at higher resolution than is present in any given image. Furthermore, although the changes in the diffraction behaviour are small they should be sufficient to cause noticeable changes in a Fresnel image series, since the fundamental reason

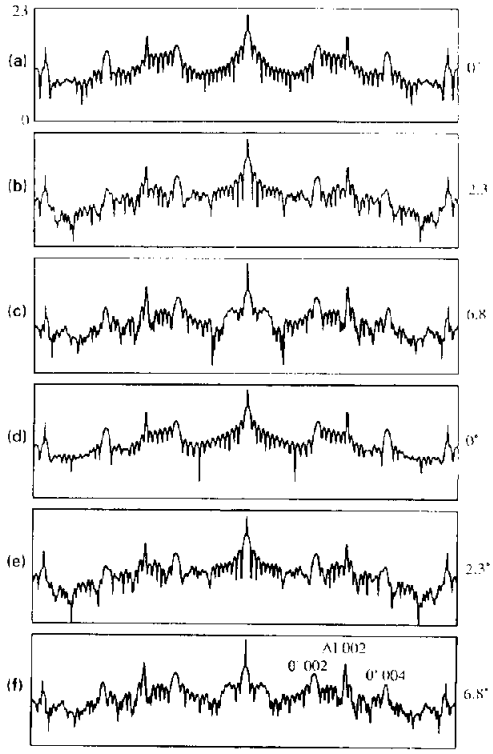

Fig. 2. As for fig. 1, but now at 50 kV.

for the sensitivity of the Fresnel method has its origins in the way in which the effect of such differences can be amplified using the angularly dependent phase changes caused by changing the defocus. A careful examination of the relative magnitudes of the graphs indicates that the greatest difference between the diffraction behaviour of the discrete and diffuse interface models occurs at the [100] zone axis. Now we need to examine some images to see the changes these differences cause in the fringe profiles. Figs. 5a and 5b show focal series for tilts of 0° and 9° respectively, as calculated at 50 kV for an objective aperture of semi-angle 4.6 mrad (0.25 times $2\theta_B$ for the θ' 002 reflection). Differences between the image series for the discrete and diffuse interfaced models are evident both in the contrast and in the form of the fringes for both tilts at this voltage despite the changes in the dynamical scattering which would be expected. An image such as that at Gaussian defocus for the calculations at zero tilt shows contrast differences of 15% between the two models, which are large enough to be useful experimentally. The "difference" diffraction patterns of fig. 4 show that changes should also be present at 200 kV; differences are indeed evident in the 200 kV images at [100] in fig. 5c (the aperture semi-angle is now 0.53 times $2\theta_B$ for θ' 002 at 200 kV). The increased sensitivity of the simulations to the compositional abruptness at the atomic level appears encouraging, so we now turn to an analysis of an experimental series taken at 200 kV.

4. Experimental

A disc of Al–4wt%Cu was solution treated at 530°C for 2 h and water-quenched. It was then aged for $5\frac{1}{2}$ hours at 217°C (above the θ'' solvus so that θ' formed directly from the supersaturated solid solution) and ground to a thickness of 100 μm. 3 mm foils were punched and electropolished using a solution of 25% nitric acid and 75% methanol at −30°C. At the low ageing temperature used the platelets were found to be well separated and homogeneously distributed. The particular θ' platelet chosen for examination was

known to extend through the entire foil thickness and examination of the specimen edge showed that neither matrix nor precipitate had thinned preferentially. Examination of the platelet in dark field using a θ' reflection confirmed the absence of growth ledges on the precipitate in the thinner regions of the foil that were used for analysis.

An experimental through-focal series of 21 images was taken at a magnification of 200 000 using a JEOL 2000FX microscope ($C_s = 2.3$ mm) operated at 200 kV, with focal steps of 120 nm and 2.8 s exposure times. The specimen was tilted to a systematic row 3.6° from $\langle 001 \rangle_{Al}$, keeping the plane of the interface between the θ' and the matrix close to the incident beam direction. An objective aperture of semi-angle 3.48 mrad (Airy disc diameter 0.878 nm) was used, and the convergence semi-angle was measured as 0.2 mrad from the diffraction pattern. For comparison, $2\theta_B$ for the θ' 002 reflection is at 8.64 mrad at 200 kV.

One image from the experimental series, at a defocus of 480 nm, is shown in fig. 6. The large number of fringes visible parallel to the interface can be noted and is indicative of the low beam convergence of 0.2 mrad used. A qualitative examination of the image series suggested that although care had been taken to ensure a tilt that

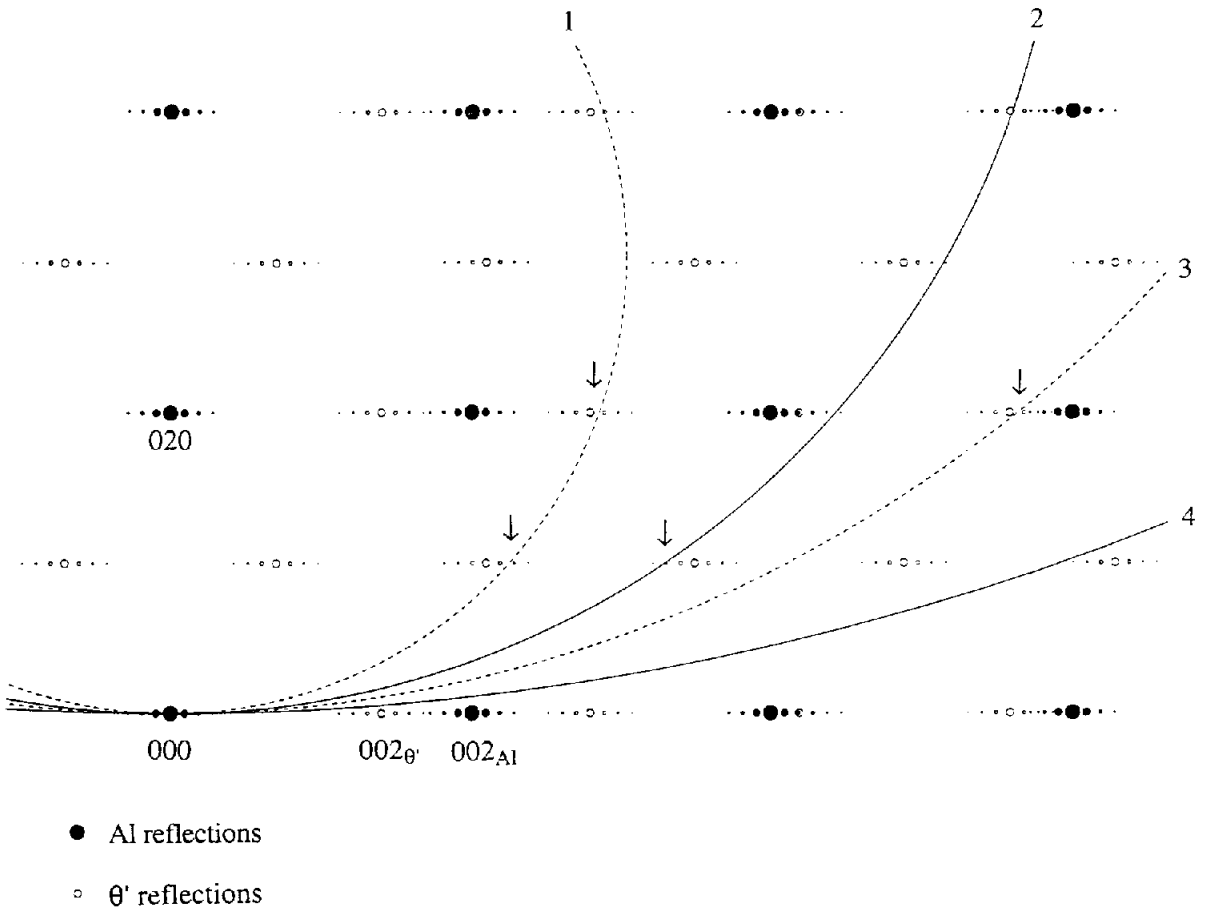

Fig. 3. Schematic diagram of diffraction pattern showing subsidiary maxima of θ' reflections for platelet $7\frac{1}{2}$ unit cells thick. Circles indicate positions of Ewald sphere intersections with zeroth Laue zone for tilts of 2.1° and 6.4° at 200 kV (2 and 4), and 2.3° and 6.8° at 50 kV (1 and 3). Examples of θ' reflections whose double diffraction would be expected to influence the shape of the $(000)_{\theta'}$ reflection are arrowed.

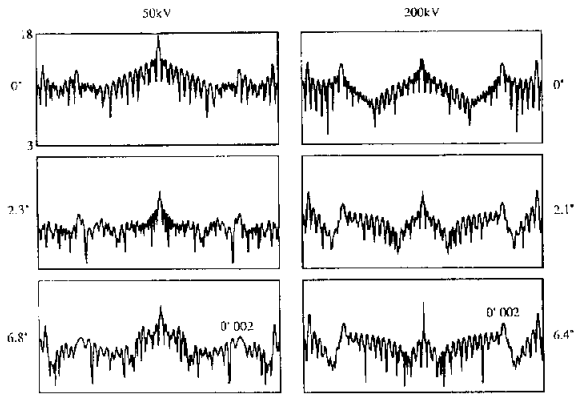

Fig. 4. Absolute differences between diffraction patterns calculated for two models and shown in figs. 1 and 2. Graphs are again plotted on natural log scale, and tilts from [100] are indicated.

was close to the Laue orientation, the local tilt of the θ' platelet about [010] could be seen to change slightly along its length. The specimen thickness of the area chosen for analysis was accurately characterised as 47.5 ± 2.0 nm using $(g, 4g)$ and $(g, 5g)$ weak-beam thickness fringes with $g = 200$. Every other image in the series was digitised using an Eikonix densitometer at a resolution of 14 μm/pixel on the plate (0.07 nm/pixel on the specimen) and corrected for both emulsion and densitometer response using the SEMPER image processing system on a Silicon Graphics Iris. The fringes were projected parallel to the interfaces along a direction found accurately by cross-correlating rows of pixels. Care was taken to ensure that the average specimen thickness across the fringes remained constant. The resulting 1D profiles were divided by the slowly varying background and scaled to an incident electron intensity of 1 given by the intensity in the vacuum close to the specimen edge. These profiles are shown in fig. 7a. Fig. 7b shows the same profiles after making them symmetrical by flipping them horizontally – although this approach has worked previously for less dynamical situations, it is potentially misleading here be-

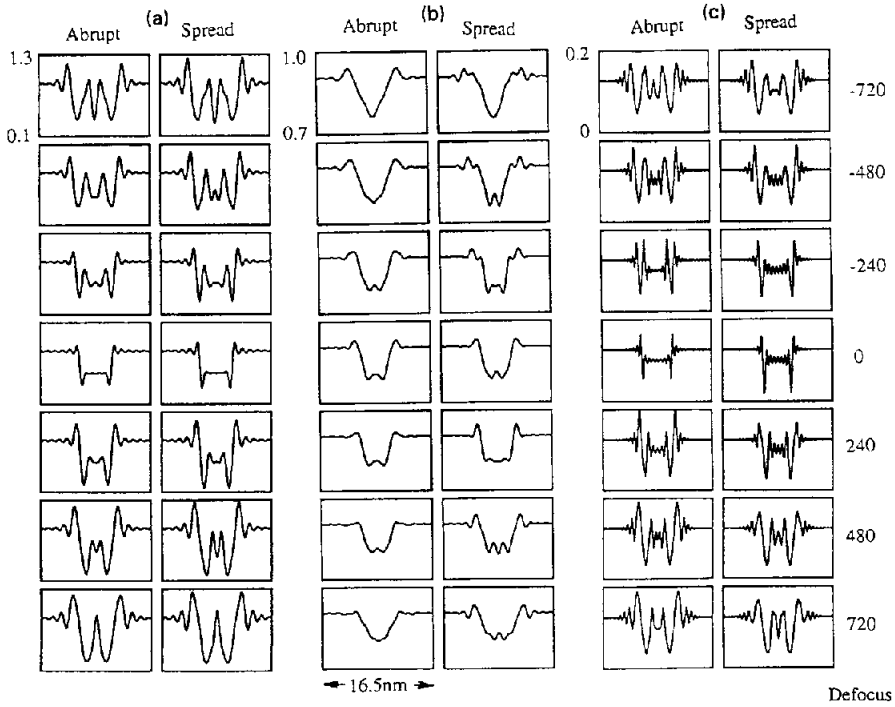

Fig. 5. Focal series calculated for typical experimental parameters at defoci indicated: (a) 50 kV, zero tilt from [100]; (b) 50 kV, 9° tilt from [100]; (c) 200 kV, zero tilt from [100].

cause the form of the fringes is so sensitive to crystal tilt and often changes across the middle of the profiles. Even at this fairly systematic row orientation, the background intensity of the aluminium still varies with specimen thickness. This can be seen from the simulated graphs in fig. 8, which show the zero beam amplitude as a function of specimen thickness for different orientations. The standard approach of extrapolating the experimental fringe spacing to zero defocus suggests that the plate contains approximately 15 Cu

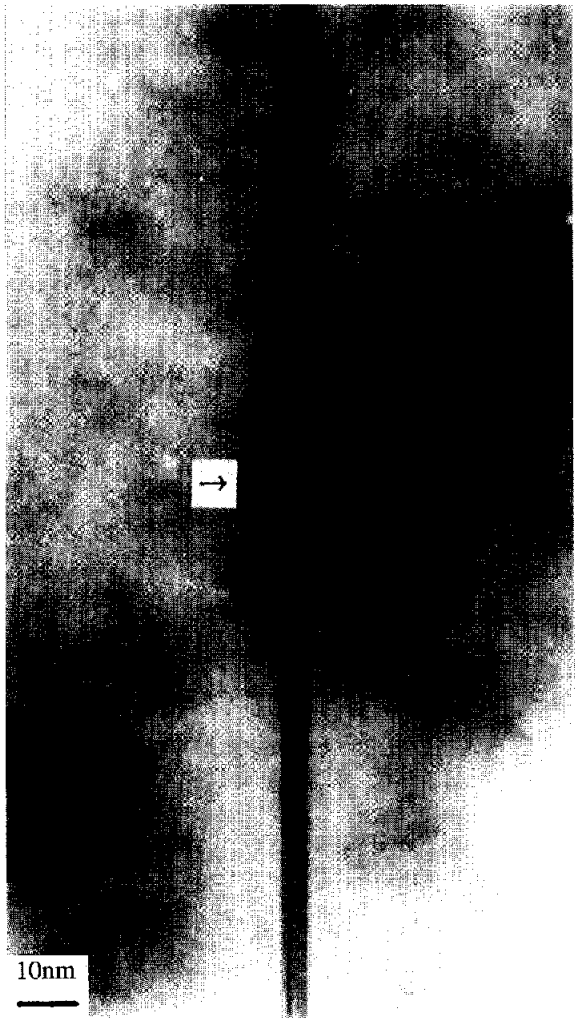

Fig. 6. Image from through-focal series of θ′ precipitate, at approximately 480 nm overfocus. Region subsequently analysed, at 47.5 nm specimen thickness, is arrowed.

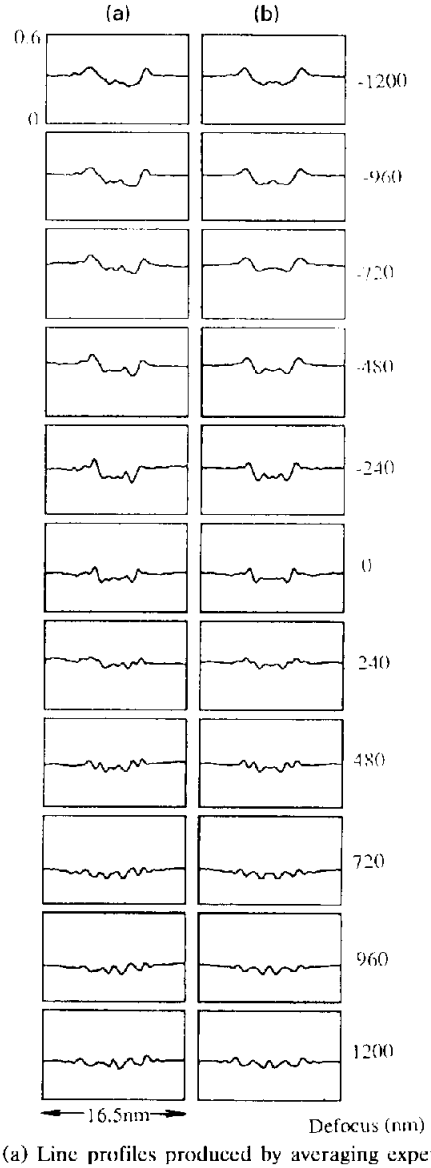

Fig. 7. (a) Line profiles produced by averaging experimental images parallel to the interface, at 47.5 nm thickness. Profiles are corrected for emulsion and densitometer response, and are plotted on a scale where incident intensity is 1. (b) The same profiles, processed to make them symmetrical. Note contrast form changes from (a).

layers (each Cu layer is associated with a single half-unit cell of θ′). Platelets of width 14, 15 and 16 Cu layers are expected to be of interstitial, vacancy and interstitial character in the matrix with misfits of 0.3%, 2.4% and 4.2%, respectively

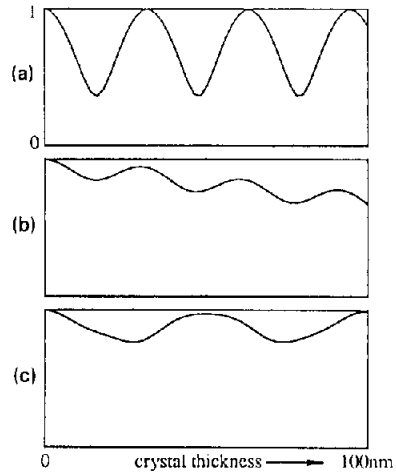

Fig. 8. Amplitude of zero beam, simulated as a function of crystal thickness and plotted with crystal at (a) [100] zone axis; (b) Laue orientation 3.6° from [100]; (c) 0.18° tilt from Laue orientation of (b).

[6]. For comparatively wide plates such as these the magnitudes of the contrast from each interface are independent for lower defoci, and the width of a plate should alter only the detailed form of the fringes as a function of changes in the dynamical scattering as discussed above.

It is especially interesting that the experimental background level is about 0.3, indicating that experimentally 70% of incident electrons have been scattered out of the objective aperture used. It is thus disturbing that simulations calculated for the experimental conditions show a background intensity of about 0.7 to 0.8 rather than the experimental value of 0.3. The multislice calculations treat the contribution to absorption only due to elastic scattering by the crystal, but no reasonable values of V_0', or V_g' would make the fit much better. The observation that many more electrons can be scattered out of a given objective aperture than theory predicts has been reported for ion-thinned semiconductors [7] and was then attributed, at least partly, to the effects of amorphous contamination at the foil surfaces. The Al–Cu specimen used for the experimental series had been examined in the microscope several times, contamination was visible at the specimen edge and a similar origin for the intensity loss is not inconceivable. To first order, the most straightforward treatment for comparing experiment and theory seemed to be to scale the background level of all the simulations to the experimental value of 0.3. On this basis it is assumed that there is no differential contribution to the platelet contrast due to the extra electrons scattered out of the aperture. Assuming that this is a reasonable approach to take, the value of the experimental tilt should be provided by the standard approach of plotting fringe and platelet contrast as a function of defocus [1], bearing in mind also that at this orientation the contrast is likely to be more sensitive to diffraction than to Fresnel effects.

Fig. 9 shows simulated defocus series for the accurate experimental thickness and for a range of crystal tilts about [010] at an angle of 3.6° from (100) about [001]. It was known from a preliminary set of simulations that both the magnitude and the form of the contrast were more sensitive to crystal tilt than to specimen thickness, and that at this orientation the fringes should be fairly insensitive to compositional spread at high defocus. It is clear from the images that the experimental fringe contrast is of opposite sense to that of the simulations at the Laue orientation, and this indicates that the local crystal tilt must be at least 0.04° (1/8 of the 002 Bragg angle). From the Laue orientation, the simulated contrast reverses and increases in magnitude as the Al 002 Bragg condition is approached. Experimentally the only region of the platelet that showed symmetrical contrast was in the buckled area near to the foil edge and unsuitable for analysis. A qualitative upper limit on the experimental crystal tilt is imposed by the fact that, at the experimental thickness, the contrast is still far from being at the 002 Bragg condition.

Fig. 10 shows the graphs of experimental and simulated contrast as a function of defocus. The definitions of contrast used here are included in the figure. The high gradient in the experimental curve with change in focus can be noted together with the tendency for the contrast to decrease towards the overfocus side. Strangely it is the Laue condition that seems to produce the closest match of contrast trends with defocus, however the sense of the contrast is clearly incorrect (see

fig. 9). The magnitude of the contrast seems to indicate a tilt of between 1/8 and 1/4 times 002 Bragg, but the trends with defocus in the graphs point to a slightly higher tilt. Fig. 11 shows that convergence decreases the fringe contrast equally on both sides of zero defocus, and does not introduce the observed gradient.

The high general gradient with defocus in the contrast changes observed experimentally can of course be accounted for by a slight change in the experimental crystal tilt over the image series. In considering the sensitivity of the approach we are

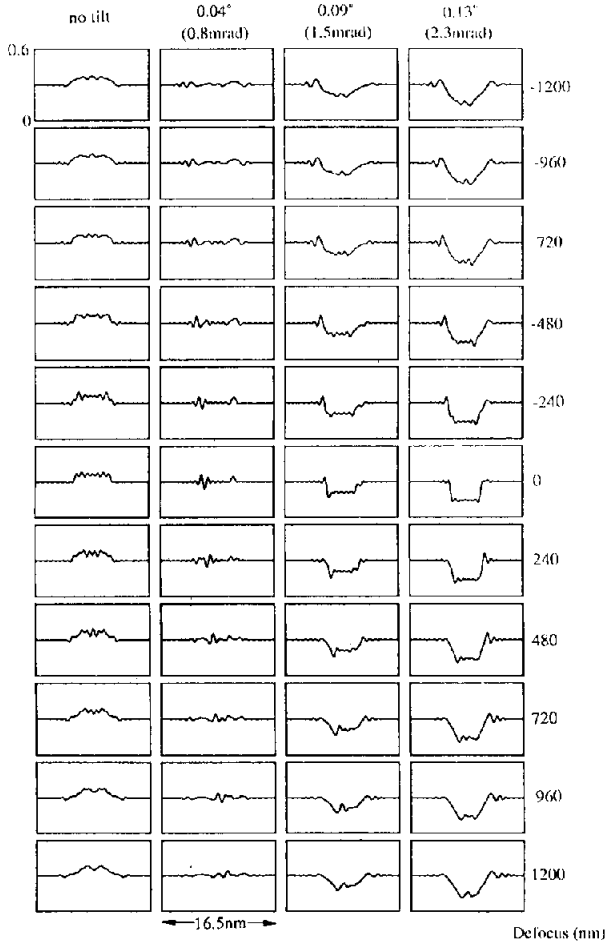

Fig. 9. Simulated Fresnel fringes from 4.4 nm thick θ′ precipitate. Defoci and tilts from Laue orientation of fig. 8b are shown.

examining, it is interesting to note that the lateral shift of opposite faces of the crystal, and therefore also the accuracy in the projected potential necessary for a tilt of 1/16 of an Al 002 Bragg angle at 200 kV is only 0.018 nm at the experimental thickness of 47.5 nm. A reason why the level of the contrast is slightly lower than expected may be due to differential scattering of the extra electrons scattered out of the aperture, but the major surprise is that the experimental contrast *variations* with defocus are larger than those of any of the simulations. This implies either that a higher proportion of non-contrast retaining electrons have been scattered out of the aperture or that the fundamental potentials derived on the basis of Doyle and Turner's data [5] are incorrect. Similar anomalies have been observed for an oxide layer on silicon [8], where the fringe contrast of the interface was found to be higher when using a 5.8 mrad than a 1.9 mrad objective aperture. It is worth highlighting the distinction between the analysis of an isolated layer and a periodically repeating unit. For a W/Si multilayer, although the experimental contrast level was also low when compared with predictions, strong interference effects associated with a repeating structure of small wavelength ensured that the form of the contrast could be analysed uniquely [9]. This is not possible here and the reason for the lack of a reasonable match between the experimental and theoretically predicted intensity would seem to be required before the contrast can be assessed with any confidence.

It is however interesting that the experimental contrast at one interface behaves, in form, more like the simulations than does the other. An interesting but tentative suggestion for the reason for such an inconsistency comes from the fact that only one side of the θ′ plate shows a growth ledge (at about double the specimen thickness of the area analysed), and a diffusion gradient of Cu to this ledge may have frozen into the structure on cooling. Other feasible explanations for such an inconsistency include, however, a change of plane spacing to accommodate elastic misfit, impurity segregation to the boundaries, or the effect of foil preparation introducing a free surface, so we are again unable to come to an unequivocal

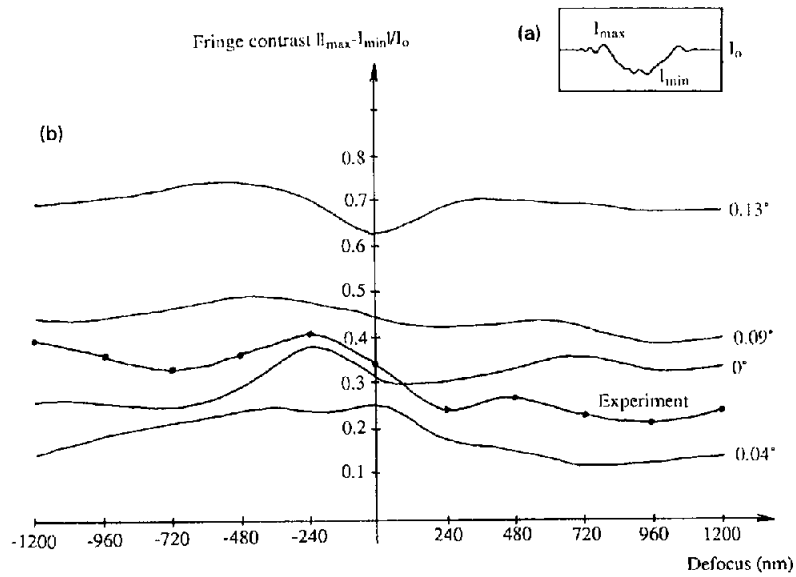

Fig. 10. (a) Definition of parameters used to describe fringe contrast in this paper. (b) Graphs of fringe contrast as a function of defocus for experimental and simulated profiles. Tilts from the Laue orientation are indicated.

conclusion about any difference in structure for the two interfaces.

5. Discussion and conclusion

The theoretical behaviour of diffraction patterns to be expected for θ' precipitates in Al–4wt%Cu has been described as a function of crystal tilt, accelerating voltage and compositional spread at the θ' interfaces. The aim of the work was to investigate the sensitivity of Fresnel contrast analysis to compositional spread in the presence of dynamical effects. The simulations were also obtained for a range of tilts close to a major zone axis to examine the effects of changes in the dynamical contributions associated with the [001]

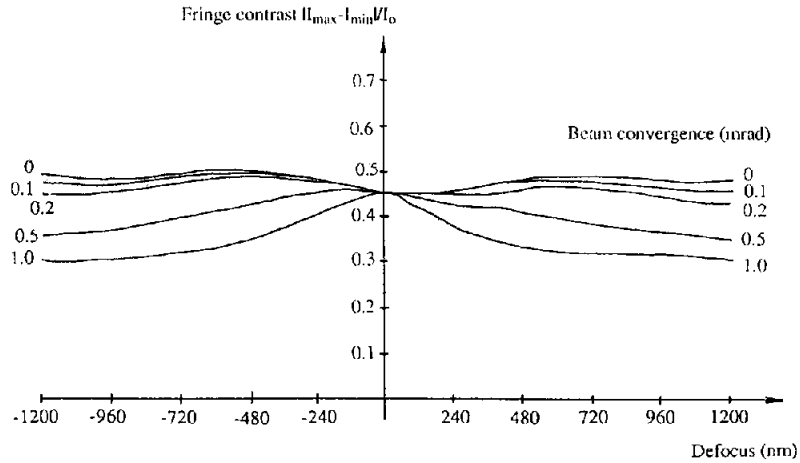

Fig. 11. Fringe contrast as a function of beam convergence for a tilt of 0.09° from the Laue orientation.

spread of the θ' reflection. It was found that diffraction patterns at all crystal tilts showed differences between the diffuse and abruptly interfaced models. While we did not find it surprising that a weakly diffracting condition, as used in standard Fresnel analyses to date proved to be sensitive to the composition, it is interesting that differences were also visible in the images calculated close to a zone axis and with relatively strong non-systematic diffraction. The work described has shown that, to varying degrees, the contrast should be sensitive to the composition profile at all of the tilts examined and we have found no reason to suggest that an analysis carried out using a small objective aperture should not be sensitive to compositional spread for interface characterisation to the atomic level.

Experimentally, a symmetric Laue orientation is to be preferred over other orientations given that the contrast changes in form as the interface is tilted from the vertical. This point has been illustrated in the characterisation of a preliminary experimental series. The primary conclusions of the experimental part of our study are as follows. An anomalously large number of electrons was found to have been scattered out of the aperture at the specimen thickness examined. This was only modelled to first order and the inadequacy of the assumptions made is exemplified by the inability of the simulations to reproduce the large contrast variations experimentally observed on changing the defocus, even assuming a change of experimental tilt through the series. These variations probably indicate that scattering out of the aperture by processes other than elastic scattering by the crystal has not been included correctly in our simplistic treatment. The effects are caused by contamination layers at the specimen foil surfaces, and cannot be accounted for using conventionally reasonable absorption parameters [7]. It should further be emphasised that including energy loss processes into the calculations and examining the contrast contributed by such energy loss electrons would have little effect. Our current problem in the interpretation would still have been present even if energy filtering had been used. It thus appears that any understanding of the differences in the experimentally observed contrast behaviour with that simulated would require a more full treatment of the electrons lost from the aperture than the simple scaling approach applied here. If, for example, a degree of knock-on damage in the Al caused it to scatter more, diffusely, out of the aperture than did the platelets then the observed trends could be qualitatively explained. The theoretical and experimental image profiles showed broad similarities but their form could not be fitted exactly. It would appear that this preliminary experimental study has simply highlighted the importance of using clean and undamaged samples when attempting to make quantitative interpretations of the image contrast.

Acknowledgements

We would like to thank Professor C.J. Humphreys for the provision of laboratory facilities and G.E.C. for financial support.

References

[1] F.M. Ross and W.M. Stobbs, Phil. Mag. A 63 (1991) 1.
[2] F.M. Ross and W.M. Stobbs, Ultramicroscopy 36 (1991) 331.
[3] K.M. Knowles, F.M. Ross and W.M. Stobbs, Paper presented at EMAG 87 Analytical Electron Microscopy Workshop, Manchester (1987) p. 55.
[4] F.M. Ross, PhD Thesis, Cambridge University (1988).
[5] P.A. Doyle and P.S. Turner, Acta Cryst. A 24 (1968) 390.
[6] W.M. Stobbs and G.R. Purdy, Acta Met. 26 (1978) 1069.
[7] A.S. Dobson, A.R. Preston and W.M. Stobbs, Inst. Phys. Conf. Ser. No. 119, Paper presented at EMAG 91, Bristol (1991) p. 449.
[8] F.M. Ross and W.M. Stobbs, Phil. Mag. A 63 (1991) 37.
[9] W.C. Shih and W.M. Stobbs, Ultramicroscopy 32 (1990) 219.